



HAL
open science

Modélisation multiphysique des matériaux à bas point de Curie magnétique

Hakim Oueslati, Didier Trichet, Guillaume Wasselynck, Simon Morville

► **To cite this version:**

Hakim Oueslati, Didier Trichet, Guillaume Wasselynck, Simon Morville. Modélisation multiphysique des matériaux à bas point de Curie magnétique. Symposium du Génie Electrique, L2ep, Jul 2023, Lille, France. hal-04526792

HAL Id: hal-04526792

<https://hal.science/hal-04526792v1>

Submitted on 3 Jul 2024

HAL is a multi-disciplinary open access archive for the deposit and dissemination of scientific research documents, whether they are published or not. The documents may come from teaching and research institutions in France or abroad, or from public or private research centers.

L'archive ouverte pluridisciplinaire **HAL**, est destinée au dépôt et à la diffusion de documents scientifiques de niveau recherche, publiés ou non, émanant des établissements d'enseignement et de recherche français ou étrangers, des laboratoires publics ou privés.

Multiphysics Modelling of Low Magnetic Curie Point Materials

Hakim Oueslati^{1,2}, Didier Trichet¹, Guillaume Wasselynck¹, and Simon Morville²

¹ Nantes University, Institut de Recherche en Energie Electrique de Nantes Atlantique, 37, Bd de l'université, Saint-Nazaire 44612, France

² Institut de Recherche Technologique Jules Verne, 1 Mail des 20 000 lieux, 44340 Bouguenais, France

Controlled Curie point materials are considered as innovative materials due to their property of abrupt magnetic extinction when their temperature exceeds a specific threshold. A coupled electromagnetic and thermal FEM model for induction heating of a magnetic material with a low Curie point temperature is presented.

The simulation results allow a comparison of the induced power density for different temperatures.

Curie temperature, Ferromagnetism, Finite Element method.

I. INTRODUCTION

IN recent years, metallurgists have developed so-called "controlled Curie point" materials. These materials have the property of being magnetically extinguished when their temperature exceeds a specific threshold. The transfer of power by electromagnetic induction could be strongly reduced in these regions, which opens the door to a thermal self-regulation of the process without sensors and only in the zones of interest (low energy).

This threshold is usually around $800^{\circ}C$ for steel, but there are now materials whose threshold is determined during manufacture over the range from ambient to $800^{\circ}C$. This temperature range opens interesting perspectives for the elaboration of thermoplastic (preforming, forming, welding, ...) and thermoset composites (polymerisation, recycling, ...).

The main objective is to evaluate the potential of integrating these materials in the elaboration processes of glass or carbon fibre composites widely used in aeronautical and space industries.

II. MATHEMATICAL MODELLING

The magnetic vector potential formulation in magnetoquasistatics is written as follows [1] :

$$-\nabla \cdot (\nu \nabla \mathbf{A}) + \sigma \left(\frac{\partial \mathbf{A}}{\partial t} + \nabla V \right) = \mathbf{J}_s, \quad (1)$$

where V is the scalar electric potential [V].

In order to solve this partial differential equation, the finite element method is used. Knowing that ferromagnetic (Curie point) materials are doubly non-linear in magnetic field, thus in magnetic vector potential, and in temperature, a method for solving a system of non-linear equations must be adapted to the finite element code [2]. In order to simplify the calculations and given the long simulation times, a 2D geometry in axisymmetric configuration is chosen. With axisymmetric hypothesis, magnetoc vector potentiel \mathbf{A} and source current density \mathbf{J}_s have only one component in the azimuthal direction [3].

$$\mathbf{A} = (0, A_{\theta}, 0) ; \mathbf{J}_s = (0, J_{s\theta}, 0) \quad (2)$$

The development of (1) in $[r,z]$ plan yields to the expression below :

$$-\nabla \cdot \left(\frac{\nu}{r} \nabla (r A_{\theta}) \right) + \sigma \frac{\partial (r A_{\theta})}{\partial t} = J_{s\theta}, \quad (3)$$

In this case, the finite element matrix formulation is [4] :

$$[K][A_{\theta}] + [M] \frac{\partial [A_{\theta}]}{\partial t} = [F], \quad (4)$$

where $[K]$ and $[M]$ are respectively the stiffness and mass matrices. The time derivative of the formulation in A can be approximated by the Euler method, which is a method for solving ordinary differential equations. In our case, an implicit Euler method was adapted to the finite element code and it leads us to a system of non linear equations :

$$[K_1(A_{\theta(t_{j+1})})][A_{\theta}]_{t_{j+1}} = [FT]_{(t_{j+1})} \quad (5)$$

with $[K_1(A_{\theta(t_{j+1})})] = [K] + \frac{[M]}{\Delta t_j}$ and $[FT]_{(t_{j+1})} = [F]_{(t_{j+1})} + \frac{[M]}{\Delta t_j} + [A_{\theta}]_{(t_j)}$.

Due to the non-linearity of the $[K_1]$ matrix in magnetic vector potential \mathbf{A} , the Newton-Raphson method can be used to linearise the equations and by combining it with a method of solving the system of linear equations such as the biconjugate gradient method, the values of the nodal potentials are computed.

$$\left([K_1] + \frac{\partial [K]}{\partial A_{\theta(t_{j+1})}^T} [A_{\theta}]_{(t_{j+1})}^{(n)} \right) \Delta A_{(t_{j+1})}^{(n+1)} = [FT]_{(t_{j+1})} - [K_1][A_{\theta}]_{(t_{j+1})}^{(n)} \quad (6)$$

The thermal equation will be presented in the final paper.

III. NUMERICAL SIMULATION

III-A. Material

Ferromagnetic $Fe - Ni - Cr$ austenitic alloys with less than 50%Ni have Curie point T_c varying continuously with composition between $0^{\circ}C$ and $500^{\circ}C$ [5]. The material chosen for the numerical simulation is a ferromagnetic material with a Curie temperature $T_c = 260^{\circ}C$. The magnetisation curve $B(H)$ decreases progressively (Fig. 1) as the temperature T approaches T_c , and the closer T is to T_c , the smaller $B(H)$ becomes. It should be noted that the permeabilities of these materials are high (μ_r of the order of 20,000), which potentially favours the generation of induced currents (source of heat). As can be seen in the Fig. 1, the magnetic field does not exceed 2.5×10^4 A/m and is still far from magnetic saturation. It is therefore necessary to use extrapolation methods to extrapolate the experimental values to the saturation point (H_s, B_s) . From this point, the permeability becomes equal to $\mu_0 = 4.\pi.10^{-7}$ H/m. There are many methods of extrapolation but for the following, we have opted for the Exponential Law Extrapolation (ELE) which has proved to be more accurate than the others. [6]

Fig. 1 shows the B(H) curves of the material at different temperatures. It can be seen that when the Curie temperature is exceeded, the relative magnetic permeability becomes equal to 1 and $B = \mu_0 \times H$.

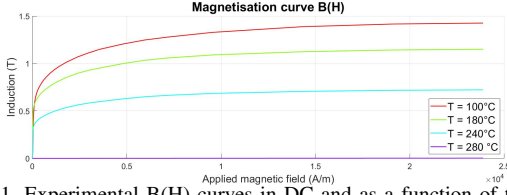


FIG. 1. Experimental B(H) curves in DC and as a function of the measuring temperature of a ferromagnetic material

III-B. Numerical results

The Newton-Raphson method is used to linearise a system of non-linear equations. In this case, the number of iterations of the method is 100 and the tolerance is set at 10^{-4} .

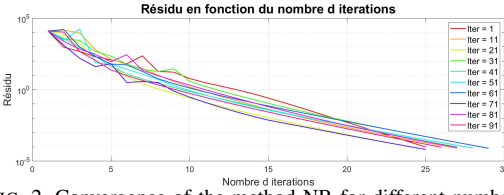


FIG. 2. Convergence of the method NR for different numbers of time iterations

The volumic power density is evaluated according to the following formula :

$$p_i = \mathbf{J}_i \cdot \mathbf{E} = \frac{1}{\sigma} \mathbf{J}_i^2 = \sigma \left(\frac{\partial \mathbf{A}_\theta}{\partial t} \right)^2 \quad (7)$$

The total induced power is the average power over all elements and therefore depends on the geometry. It also depends on the density of the source current feeding the inductor.

If the density increases, the induced power increases. As it can be seen from the table I, the total induced power decreases considerably as the Curie point is reached.

TABLEAU I. Evolution of the total induced power for different temperatures with a frequency equal to 20kHz

	$T = 100^\circ\text{C}$	$T = 180^\circ\text{C}$	$T = 240^\circ\text{C}$	$T = 280^\circ\text{C}$
$P_{ind}(W)$	2342.1	2317.9	2432.8	67.590

IV. ANALYTICAL VALIDATION

A validation step is often necessary to show the relevance of the implemented model. In our case, an analytical solution is studied and compared to the obtained numerical solution [7].

$$A^{(3)}(r, z) = \mu i_0 \int_0^\infty \left(\frac{1}{\alpha^3} \right) I(r_2, r_1) J_1(\alpha r) [\exp(-\alpha l_1) - \exp(-\alpha l_2)] \times \left[\frac{\alpha(\alpha_1 + \alpha_2) \exp(2\alpha_1 c) \exp(\alpha_1 z) + \alpha(\alpha_1 - \alpha_2) \exp(-\alpha_1 z)}{(\alpha - \alpha_1)(\alpha_1 - \alpha_2) + (\alpha + \alpha_1)(\alpha_2 + \alpha_1) \exp(2\alpha_1 c)} \right] d\alpha \quad (8)$$

where $\alpha_i \equiv (\alpha^2 + j\omega\mu\sigma_i)^{\frac{1}{2}}$.

This formulation is only valid in the magnetoharmonic case and for a relative magnetic permeability equal to 1.

Fig. 3 shows the evolution of the induced current density as a function of the radial component r at an axial component z equal to the skin thickness δ , for the analytical solution as well as for the numerical solution obtained by the finite element method. We can see that the two curves overlap, which allows us to validate the numerical results obtained in the magnetoharmonic case.

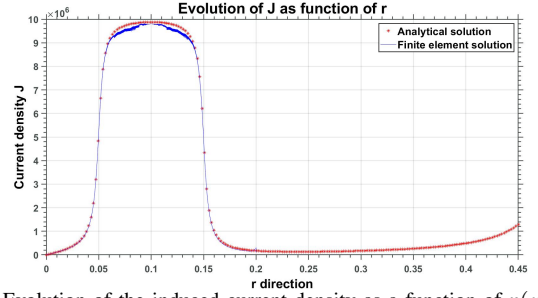


FIG. 3. Evolution of the induced current density as a function of r ($z = \delta$)

TABLEAU II. Validation of the numerical results with the analytical solution

Puissance totale induite (FEM) - P_{fem}	878[W]
Puissance totale induite (solution analytique) - P_{an}	905[W]
$\frac{P_{fem} - P_{an}}{P_{fem}} \times 100$	3.05%

According to the table II, there is a difference of 3% between the total induced power calculated analytically and numerically which is sufficient to validate the model in the magnetoharmonic case.

V. CONCLUSION

The objective of this paper is to have a complete model for Curie point materials taking into account the multi-scale aspect of time between the thermal model and the electromagnetic model and also taking into account the skin effect since at the passage of the Curie point, the relative magnetic permeability tends abruptly to 1 which leads to meshing difficulties due to the sudden change of the skin thickness.

In the final paper, the application of this method to get thermal self-regulation will be presented. This requires a magnetothermal coupling (strong or weak), a good choice of the numerical methods used following a good management of the sudden change of magnetic state in the vicinity of the Curie point and the consideration of the non-linearity of the parameters as a function of the temperature.

VI. REFERENCES

- [1] M. Ndiaye, "Outils de modélisation et règles de conception globale de procédés d'assemblage de composites thermoplastiques par induction électromagnétique", *Ph.D. dissertation*, Nantes Université, 2022.
- [2] T. Todaka, T. Kishino, and M. Enokizono, "Low Curie temperature material for induction heating self-temperature controlling system", *Journal of Magnetism and Magnetic Materials* 320, e702-e707, 2008.
- [3] Z. Oudni, H. Mohellebi, M. Féliachi, "Effect of Aluminum Layer on Induction Heating Control Case Study Using Finite Elements Method", *Journal of electrical systems*, 2009.
- [4] P. Ferroillat, "Développement de formulations éléments finis 3D en potentiel vecteur magnétique : application aux machines asynchrones en mouvement", *Ph.D. dissertation*, Université Grenoble Alpes, 2015.
- [5] A. Demier, J. Giusti, S. Naudin, B. Oville, P. Perichon, F. Petit, T. Waeckerle, and T. Wery, "Etude magnétothermique d'un alliage à bas point de Curie en cuisson par induction", *Symposium de Génie Electrique*, 2016.
- [6] A. E. Umenei, Y. Melikhov, and D. C. Jiles, "Models for Extrapolation of Magnetization Data on Magnetic Cores to High Fields", *IEEE Transactions on Magnetics*, 2011.
- [7] C. V. Dodd, and W. E. Deeds, "Analytical Solutions to Eddy-Current Probe-Coil Problems", *Journal of applied physics*, Volume 39, Number 6, Mai 1968.